



Investigation of the tetraquark states $Qq\bar{Q}\bar{q}$ in the improved chromomagnetic interaction model*

Tao Guo (郭涛)¹ Jianing Li (李嘉宁)² Jiaying Zhao (赵佳星)^{3†}  Lianyi He (何联毅)² 

¹School of Mathematics and Physics, Chengdu University of Technology, Chengdu 610059, China

²Department of Physics, Tsinghua University, Beijing 100084, China

³SUBATECH, Université de Nantes, IMT Atlantique, IN2P3/CNRS, 4 rue Alfred Kastler, 44307 Nantes cedex 3, France

Abstract: In the framework of the improved chromomagnetic interaction model, we complete a systematic study of the S -wave tetraquark states $Qq\bar{Q}\bar{q}$ ($Q = c, b$, and $q = u, d, s$) with different quantum numbers: $J^{PC} = 0^{+(+)}$, $1^{+(\pm)}$, and $2^{+(+)}$. The mass spectra of tetraquark states are predicted, and the possible decay channels are analyzed by considering both the angular momentum and C -parity conservation. The recently observed hidden-charm tetraquark states with strangeness, such as $Z_{cs}(3985)^-$, $X(3960)$, and $Z_{cs}(4220)^+$, can be well explained in our model. Additionally, according to the wave function of each tetraquark state, we find that the low-lying states of each $Qq\bar{Q}\bar{q}$ configuration have a large overlap to the $Q\bar{Q}$ and $q\bar{q}$ meson basis, instead of the $Q\bar{q}$ and $q\bar{Q}$ meson basis. This indicates that one can search these tetraquark states in future experiments via the channel of $Q\bar{Q}$ and $q\bar{q}$ mesons.

Keywords: improved chromomagnetic interaction model, hidden heavy flavor tetraquark states, mass spectra and possible structures

DOI: 10.1088/1674-1137/acb87

I. INTRODUCTION

Exotic hadrons, especially the heavy flavor exotic hadrons, provide a unique tool to study the nature of the strong force and the low-energy properties of quantum chromodynamics (QCD). In addition to the open-charm tetraquark states, such as $X_{0,1}(2900)^0$ [1] and $T_{cc}(3875)^+$ [2], dozens of hidden-charm (-bottom) exotic states have been discovered since the observation of the hidden-charm state $X(3872)$ in 2003 by the Belle Collaboration [3]; see reviews [4–8]. The most fascinating and unknown aspect is the inner structure of these exotic hadrons. Theoretically, these exotic states can be mainly explained as multi-quark states, which can be molecule states or compact tetraquark states [5, 6, 9], hybrid states with the $c\bar{c}$ - g configuration [10, 11], or missing charmonium states, whose masses can be predicted by potential models but are drastically modified by thresholds [12–14], which is a kinematic effect called triangle singularity [15–17]. A clear probe to distinguish multi-quark states from hybrid states or charmonia is the charged hid-

den-charm (-bottom) exotic state [18].

In recent years, many hidden-charm (-bottom) exotic states with non-zero electric charge, such as $Z_c(3900)^+$ [19, 20], $Z_c(4025)^+$ [21], $X(4100)^+$ [22], $Z_c(4430)^+$ [23, 24], $Z_b(10610)^+$, and $Z_b(10652)^+$ [25], have been observed in experiments. From the decay, one can infer that their quark constituents are $[cu\bar{c}\bar{d}]$ or $[bub\bar{d}]$. In the meantime, charged hidden-charm tetraquark states with strangeness have also been found experimentally. In 2020, the BESIII Collaboration reported a charged hidden-charm exotic structure with strangeness based on the processes of $e^+e^- \rightarrow K^+D_s^-D^{*0}$ and $K^+D_s^*D^0$ [26]. Experimental analysis indicated that the exotic state has a mass of $(3982.5^{+1.8}_{-2.6} \pm 2.1)$ MeV and a width of $(12.8^{+5.3}_{-4.4} \pm 3.0)$ MeV, which is close to the $D_s^-D^{*0}$ and $D_s^*D^0$ thresholds. It is the first observed candidate of the charged hidden-charm tetraquark with strangeness, i.e., $[cs\bar{c}\bar{u}]$, which is named $Z_{cs}(3985)^-$. Next, the LHCb Collaboration observed an exotic state, i.e., $Z_{cs}(4000)^+$, with a mass of $(4003 \pm 6^{+4}_{-14})$ MeV and a width of $(131 \pm 15 \pm 16)$ MeV in the $J/\psi K^+$ invariant-mass spectrum [27]. Its quark com-

Received 10 February 2023; Accepted 10 April 2023; Published online 11 April 2023

* T. Guo is supported by the Scientific Research Foundation of Chengdu University of Technology (10912-KYQD2022-09557); J. Li and L. He are supported by the National Natural Science Foundation of China (11890712); J. Zhao is supported by the European Union's Horizon 2020 research and innovation program (824093 (STRONG-2020))

† E-mail: zhao-jx15@tsinghua.org.cn



Content from this work may be used under the terms of the Creative Commons Attribution 3.0 licence. Any further distribution of this work must maintain attribution to the author(s) and the title of the work, journal citation and DOI. Article funded by SCOAP³ and published under licence by Chinese Physical Society and the Institute of High Energy Physics of the Chinese Academy of Sciences and the Institute of Modern Physics of the Chinese Academy of Sciences and IOP Publishing Ltd

position is probably $[cu\bar{c}\bar{s}]$. In addition, three new candidates named $Z_{cs}(4220)^+$, $X(4685)$, and $X(4630)$ were observed with high significance in the $J/\psi K^+$ and $J/\psi\phi$ final states [27]. Very recently, a near-threshold peaking structure referred to as $X(3960)$ was discovered by the LHCb Collaboration in the $D_s^+ D_s^-$ invariant mass spectrum [28]. It is very likely a hidden-charm and hidden-strange tetraquark state, i.e., $[cs\bar{c}\bar{s}]$. The best fit gives the mass and width of $X(3960)$ as $(3955 \pm 6 \pm 22)$ MeV and $(48 \pm 17 \pm 10)$ MeV, respectively. The quantum number of this state is favored to be $I(J^{PC}) = 0(0^{++})$. In addition, a possible structure $X_0(4140)$ is observed in the $D_s^+ D_s^-$ invariant mass spectrum [28].

On the theoretical side, the mass spectra of $Qq\bar{Q}\bar{q}$ states have been predicted by the potential model [29–34], the QCD sum rule [35, 36], lattice QCD [18, 37–39], effective field theory [40–45], and the chromomagnetic interaction (CMI) model [46]. Because the CMI model [46–56] only considers the short-range chromomagnetic interaction between constituent quarks and antiquarks, it is more suitable to describe the tightly bound states. For the heavy flavor exotic state, which contains more than one light quark (antiquark) probably has a large size, the chromoelectric contribution should be included. This comes to the improved chromomagnetic interaction (ICMI) model [57–67]. The ICMI model has been used to predict the mass spectra of open heavy-flavor tetraquark states [60–62], open and hidden heavy-flavor pentaquark states [63–65], and heavy-flavor dibaryons [66, 67]. In this work, we investigated the masses, possible decay channels, and inner structures of charged and charge-neutral and open- and hidden-strange tetraquark states $Qq\bar{Q}\bar{q}$ ($Q = c, b$, and $q = u, d, s$) via the ICMI model firstly.

The remainder of this paper is organized as follows. A brief introduction of the ICMI model and the wave functions of the tetraquark $Qq\bar{Q}\bar{q}$ systems in the color-spin space is presented in Sec. II. In Sec. III, by substituting the effective masses and coupling strengths into the ICMI model, we calculate the mass spectra and wave functions of the S -wave tetraquark state $Qq\bar{Q}\bar{q}$. In addition, the related analysis of possible decay channels and the inner structures is presented in this section. We summarize the paper in Sec. IV.

II. MODEL DESCRIPTION

Analog to the meson and baryon, in this paper we study the heavy flavor tetraquark state $Qq\bar{Q}\bar{q}$. The state can be considered as the composition of a heavy quark Q , a heavy antiquark \bar{Q} , a light quark q , and a light antiquark \bar{q} in the quark model, where $Q = c, b$ and $q = u, d, s$. At the leading order, the strong interaction between constituent quarks (antiquarks) can be estimated using the one-gluon-exchange (OGE) potential. For S -wave tetraquark states, the spin-orbit angular momentum coupling

part disappears. The total potential can be reduced to two parts [68, 69]

$$V_{ij}^{\text{OGE}} = V_{ij}^{\text{cm}} + V_{ij}^{\text{ce}}, \quad (1)$$

i.e., the chromomagnetic interaction part

$$V_{ij}^{\text{cm}} = -\frac{\alpha_s \pi \delta(\mathbf{r}_{ij})}{6m_i m_j} \lambda_i^c \cdot \lambda_j^c \sigma_i \cdot \sigma_j, \quad (2)$$

and the chromoelectric interaction part

$$V_{ij}^{\text{ce}} = \frac{\alpha_s}{4r_{ij}} \lambda_i^c \cdot \lambda_j^c. \quad (3)$$

Here, the parameter m_i represents the effective mass of the i th constituent quark, α_s is the running coupling constant, $r_{ij} = |\mathbf{r}_{ij}| = |\mathbf{r}_i - \mathbf{r}_j|$ represents the spatial distance between the i -th and j -th quarks, λ_i^c ($c = 1, 2, \dots, 8$) denotes the Gell-Mann matrices acting on the color space of the i th quark, and σ_i denotes the Pauli matrices on the spin space of the i th quark. In addition, λ_i^c should be replaced with $-\lambda_i^{c*}$ if the subscript i (or j) denotes an antiquark. By integrating the spatial wave function part, we can obtain the ICMI model, which consists of the total mass of the constituent quarks, chromomagnetic interaction, and chromoelectric interaction. Therefore, the effective Hamiltonian of a tetraquark system in the ICMI model is expressed as [57]

$$H = \sum_{i=1}^4 m_i + H_{\text{cm}} + H_{\text{ce}}, \quad (4)$$

where the chromomagnetic interaction term can be expressed as

$$H_{\text{cm}} = -\sum_{i<j} v_{ij} \lambda_i^c \cdot \lambda_j^c \sigma_i \cdot \sigma_j, \quad (5)$$

and the chromoelectric interaction term can be expressed as

$$H_{\text{ce}} = -\sum_{i<j} c_{ij} \lambda_i^c \cdot \lambda_j^c. \quad (6)$$

The model parameters v_{ij} and c_{ij} incorporate the effects of the effective mass of the constituent quarks, the spatial configuration of the tetraquark system, and the running coupling constant. Considering the symmetry in the color-spin space, the chromoelectric interaction term and constituent quark mass term can be consolidated into one term [58, 63]:

$$H_0 \equiv \sum_{i=1}^4 m_i + H_{\text{ce}} = -\frac{3}{16} \sum_{i<j} m_{ij} \lambda_i^c \cdot \lambda_j^c, \quad (7)$$

with an introduced parameter $m_{ij} = m_i + m_j + 16c_{ij}/3$, which is related to the effective masses m_i and m_j of the constituent quarks and the coupling strength c_{ij} of the chromoelectric interaction. Then, the Hamiltonian of the ICMI model can be simplified as

$$H = H_0 + H_{\text{cm}}. \quad (8)$$

The above parameters, such as v_{ij} and m_{ij} , can be obtained by fitting the conventional hadron spectra.

Aiming to solve the eigen equations with the given Hamiltonian (8), we need to construct the wave function of the $Qq\bar{Q}\bar{q}$ system first. For the tetraquark states $Q_1q_2\bar{Q}_3\bar{q}_4$ where $Q = c, b$ and $q = u, d, s$, there are two types of decomposition of the wave function in the color space based on the $SU(3)$ group theory. They physically correspond to two different configurations in color space: the diquark-antidiquark configuration labeled as $|(Q_1q_2)(\bar{Q}_3\bar{q}_4)\rangle$ and the meson-meson configuration labeled as $|(Q_1\bar{Q}_3)(q_2\bar{q}_4)\rangle$ (or $|(Q_1\bar{q}_4)(q_2\bar{Q}_3)\rangle$). Taking into account the symmetry characteristics, these two configurations can be properly connected by a linear transformation. It is convenient to see that the total spin of the S -wave tetraquark states can be 0, 1, and 2; thus, the possible quantum numbers are $J^P = 0^+, 1^+, \text{ and } 2^+$. Now, we can construct the color-spin wave function for given tetraquark states. We only show the results for the $|(Q_1\bar{Q}_3)(q_2\bar{q}_4)\rangle$ basis.

For the scalar tetraquark states with $J^P = 0^+$, the color-spin basis wave functions $|\alpha_i\rangle$ ($i = 1, 2, 3, 4$) can be built as follows:

$$\begin{aligned} |\alpha_1\rangle &\equiv |(Q_1\bar{Q}_3)_0^1 \otimes (q_2\bar{q}_4)_0^1\rangle_0^1, \\ |\alpha_2\rangle &\equiv |(Q_1\bar{Q}_3)_1^1 \otimes (q_2\bar{q}_4)_1^1\rangle_0^1, \\ |\alpha_3\rangle &\equiv |(Q_1\bar{Q}_3)_0^8 \otimes (q_2\bar{q}_4)_0^8\rangle_0^1, \\ |\alpha_4\rangle &\equiv |(Q_1\bar{Q}_3)_1^8 \otimes (q_2\bar{q}_4)_1^8\rangle_0^1, \end{aligned} \quad (9)$$

where the superscripts and subscripts denote the total color and spin of $Q_1\bar{Q}_3$, the $q_2\bar{q}_4$ subsystems, and the tetraquark $Q_1q_2\bar{Q}_3\bar{q}_4$ systems, respectively. We know that the charge-neutral system has definite C -parity. Thus, if Q_1 and Q_3 , as well as q_2 and q_4 , are of the same flavor, all the above color-spin bases have a positive charge conjugation, i.e., $J^{PC} = 0^{++}$.

For the axial vector tetraquark states with quantum number $J^P = 1^+$, the color-spin basis wave functions $|\beta_i\rangle$ ($i = 1, 2, \dots, 6$) can be built as follows:

$$\begin{aligned} |\beta_1\rangle &\equiv |(Q_1\bar{Q}_3)_0^1 \otimes (q_2\bar{q}_4)_1^1\rangle_1^1, \\ |\beta_2\rangle &\equiv |(Q_1\bar{Q}_3)_1^1 \otimes (q_2\bar{q}_4)_0^1\rangle_1^1, \\ |\beta_3\rangle &\equiv |(Q_1\bar{Q}_3)_1^1 \otimes (q_2\bar{q}_4)_1^1\rangle_1^1, \end{aligned}$$

$$\begin{aligned} |\beta_4\rangle &\equiv |(Q_1\bar{Q}_3)_0^8 \otimes (q_2\bar{q}_4)_1^8\rangle_1^1, \\ |\beta_5\rangle &\equiv |(Q_1\bar{Q}_3)_1^8 \otimes (q_2\bar{q}_4)_0^8\rangle_1^1, \\ |\beta_6\rangle &\equiv |(Q_1\bar{Q}_3)_1^8 \otimes (q_2\bar{q}_4)_1^8\rangle_1^1. \end{aligned} \quad (10)$$

If Q_1 and Q_3 , as well as q_2 and q_4 , in the tetraquark $Q_1q_2\bar{Q}_3\bar{q}_4$ systems are of the same flavor, the tetraquark state has definite C -parity. The bases $|\beta_3\rangle$ and $|\beta_6\rangle$ do not change under the symmetry operation of charge conjugation, which gives $J^{PC} = 1^{++}$, while $|\beta_1\rangle$, $|\beta_2\rangle$, $|\beta_4\rangle$, and $|\beta_5\rangle$ change sign under the operation of charge conjugation, which gives $J^{PC} = 1^{+-}$.

For $J^P = 2^+$ states, the color-spin basis wave functions $|\gamma_i\rangle$ ($i = 1, 2$) are given by

$$\begin{aligned} |\gamma_1\rangle &\equiv |(Q_1\bar{Q}_3)_1^1 \otimes (q_2\bar{q}_4)_1^1\rangle_2^1, \\ |\gamma_2\rangle &\equiv |(Q_1\bar{Q}_3)_1^8 \otimes (q_2\bar{q}_4)_1^8\rangle_2^1. \end{aligned} \quad (11)$$

Similarly, each basis introduced above has definite charge conjugation if Q_1 and Q_3 , as well as q_2 and q_4 , are of the same flavor. All the above color-spin bases of the tetraquark systems have positive C -parity.

The wave function Ψ of the tetraquark state $Qq\bar{Q}\bar{q}$ with a given quantum number J^P can be expressed as the superposition of the bases shown above:

$$\Psi = \sum_{i=1}^{N_{cs}} c_i |\kappa_i\rangle, \quad (12)$$

where N_{cs} represents the number of the color-spin basis and c_i represents the amplitude for various color-spin bases, which satisfies the normalization condition $\sum_{i=1}^{N_{cs}} |c_i|^2 = 1$. Here, $|\kappa_i\rangle = |\alpha_i\rangle$, or $|\beta_i\rangle$, or $|\gamma_i\rangle$ depends on the quantum numbers. With this wave function, we can obtain the matrix form of the Hamiltonian (8), i.e., $\langle\Psi|H|\Psi\rangle$ [60]. The mass spectra of tetraquark states can be obtained by diagonalizing this matrix, and the probability $|c_i|^2$ can be used to analyze the possible decay channels of the tetraquark states.

III. RESULTS AND DISCUSSION

The parameters, such as m_{ij} and v_{ij} , in the ICMI model can be extracted by fitting the masses, especially the low-lying conventional hadrons, which have been observed in experiments. In this work, we adopt the parameters obtained in Ref. [60]. Now, we have calculated the mass spectra and wave functions of the tetraquark $Qq\bar{Q}\bar{q}$ ($Q = c, b$, and $q = u, d, s$) systems with various quantum numbers $J^P = 0^{+(+)}$, $1^{+(\pm)}$, and $2^{+(+)}$. The tetraquark state has definite C -parity as long as $Q(q)$ and $\bar{Q}(\bar{q})$ are the same flavor. The C -parity of the tetraquark state is determined by the basis, as discussed in the previous section. The tetraquark states can strongly decay into a pair of mesons. The C -parity is conserved in these processes.

For the $D\bar{D}$ ($D^*\bar{D}^*$) pair, its C -parity can be estimated as $(-1)^{L+S}$, where S represents the total spin and L represents the relative angular momentum. For other meson pairs, such as $D\bar{D}^*$ and $D_s\bar{D}_s^*$, the C -parity can be either positive or negative. The mass spectra of the tetraquark states are shown in Figs. 1–3. Additionally, for comparison, we plot all the possible meson-meson thresholds in each figure. The superposition amplitudes $\{c_i\}$ of the corresponding color-spin wave functions for each tetraquark state are listed in Tables 1–3.

A. Hidden-charm tetraquark states with $cn\bar{c}\bar{n}$, $cs\bar{c}\bar{n}$, and $cs\bar{c}\bar{s}$ configurations

1. The $cn\bar{c}\bar{n}$ configuration

The mass spectra of the tetraquark states with the $cn\bar{c}\bar{n}$ configuration are shown in Fig. 1(a). The superposition amplitudes of the corresponding wave functions are listed in Table 1(a). Hereinafter, the notation n represents a u or d quark. In our ICMI model, u and d quarks have

the same mass.

(1) There are four S -wave tetraquark states with $J^P = 0^+$ ($J^{PC} = 0^{++}$ for charge-neutral states, such as $[cu\bar{c}\bar{u}]$ and $[cd\bar{c}\bar{d}]$). Their masses are 3109.3, 3748.2, 3970.9, and 4146.5 MeV. The lowest state, i.e., 3109.3 MeV, lies slightly below the $\eta_c\pi$ threshold, and its wave function has a large fraction on the $\eta_c\pi$ basis ($c_1 = -0.99$). The 3748.2 MeV is above the $\eta_c\pi$ and $D\bar{D}$ thresholds. Considering the angular momentum and C -parity conservation (for charge-neutral states), this state is allowed to decay strongly into the mesons $\eta_c\pi$ or $D\bar{D}$. In this paper, we discuss only the S -wave decay and neglect the high-order decays, such as the P - and D -wave, which usually give a small contribution [63]. The 3970.9 MeV is above the $\eta_c\pi$, $D\bar{D}$, and $J/\psi\rho$ thresholds. Therefore, compared with 3748.2 MeV, this state has one more possible decay mode: $J/\psi\rho$. The remaining state with a large mass, i.e., 4146.5 MeV, can decay into mesons $\eta_c\pi$, $D\bar{D}$, $J/\psi\rho$, and $D^*\bar{D}^*$.

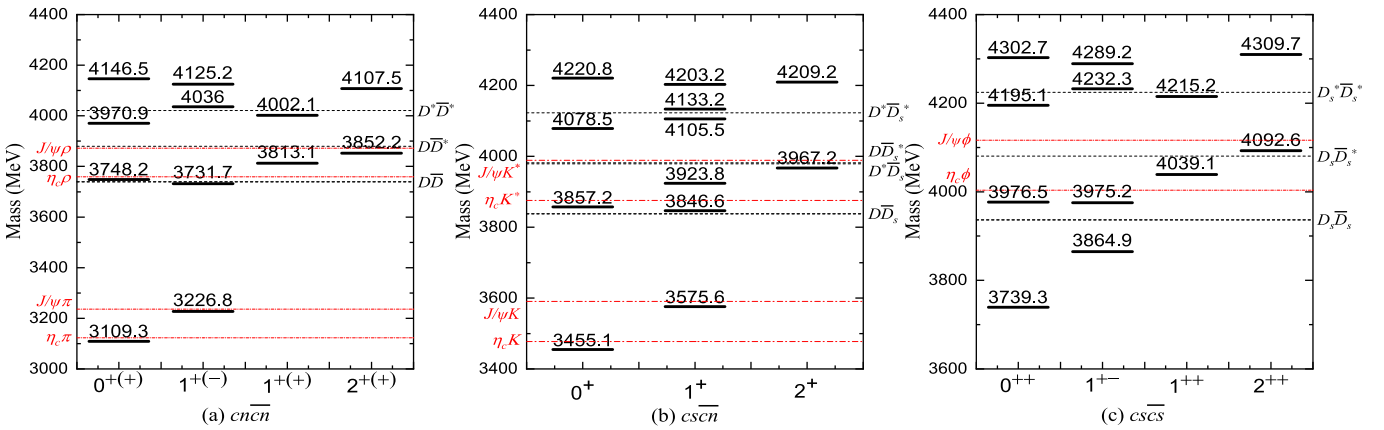


Fig. 1. (color online) Mass spectra of S -wave tetraquark states (a) $cn\bar{c}\bar{n}$ ($n = u, d$), (b) $cs\bar{c}\bar{n}$, and (c) $cs\bar{c}\bar{s}$ with different quantum numbers. The black dashed and red dot-dashed lines indicate all possible meson-meson thresholds.

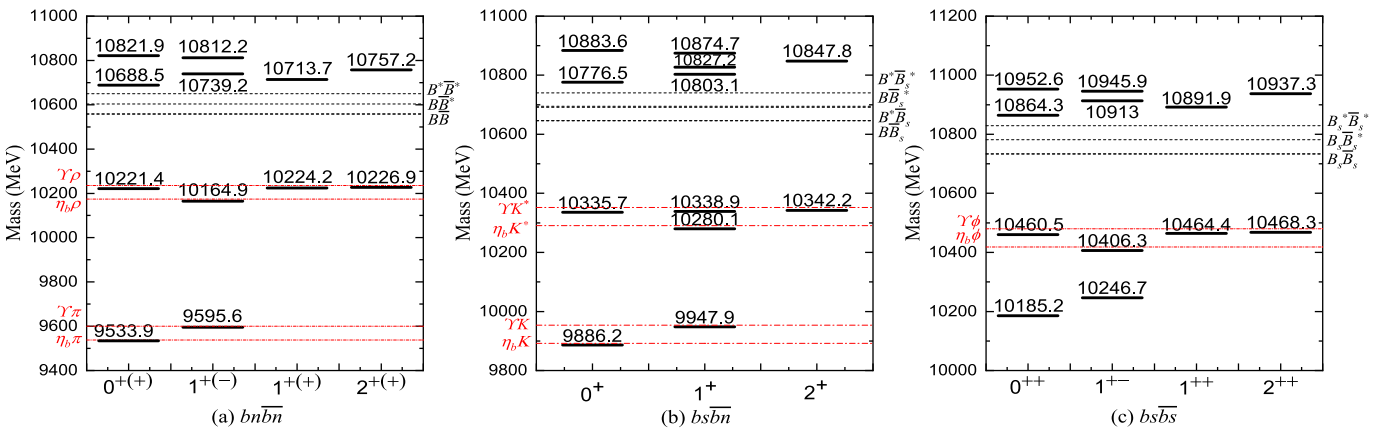


Fig. 2. (color online) Mass spectra of S -wave tetraquark states (a) $bn\bar{b}\bar{n}$ ($n = u, d$), (b) $bs\bar{b}\bar{n}$, and (c) $bs\bar{b}\bar{s}$ with different quantum numbers. The black dashed and red dot-dashed lines indicate all possible meson-meson thresholds.

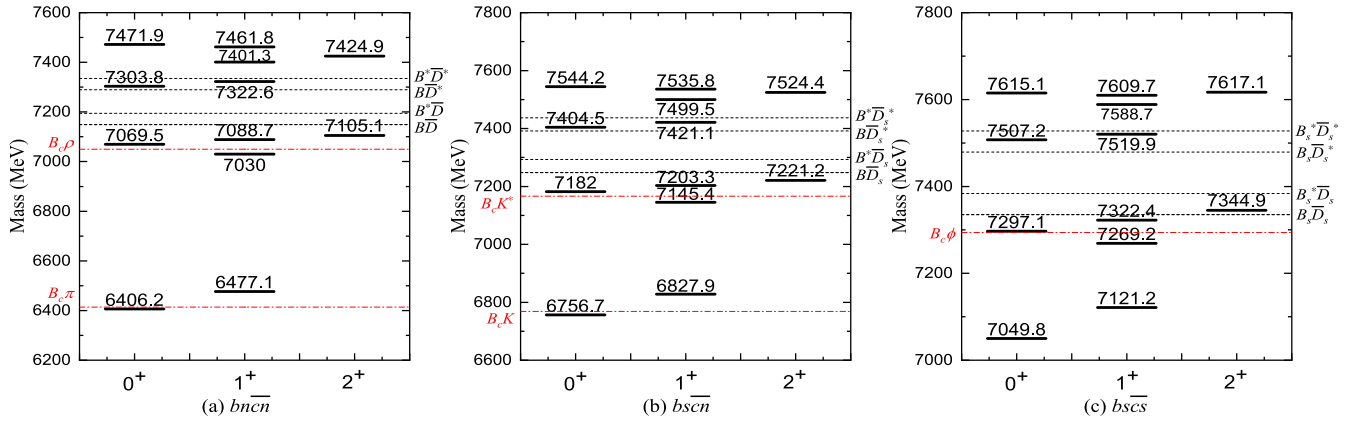


Fig. 3. (color online) Mass spectra of S -wave tetraquark states (a) $bn\bar{c}\bar{n}$ ($n = u, d$), (b) $b\bar{s}c\bar{n}$, and (c) $b\bar{s}c\bar{s}$ with different quantum numbers. The black dashed and red dot-dashed lines indicate all possible meson-meson thresholds.

(2) There are six S -wave tetraquark states with $J^P = 1^+$. Charge-neutral tetraquark states can be separated into two classes according to the C -parity. There are four S -wave tetraquark states with $J^{PC} = 1^{+-}$. The lowest state, with a mass of 3226.8 MeV, is slightly lower than the $J/\psi\pi$ threshold. Its wave function has a large fraction on the $J/\psi\pi$ basis ($c_2 = -0.99$). It can decay into J/ψ and π easily owing to the large fraction and small mass difference. Similarly, the state with a mass of 3731.7 MeV is close to the $\eta_c\rho$ threshold. The large fraction c_i indicates that it can decay into η_c and ρ easily. Additionally, it can decay into the mesons $J/\psi\pi$ (decay into $D\bar{D}$ via S -wave breaks the C -parity). The other two states, i.e., 4036.0 and 4125.2 MeV, lie above all meson-meson thresholds. Considering the conservation law in the decay process, the possible decay channels are $J/\psi\pi$, $\eta_c\rho$, and $D\bar{D}^*$. There are two other S -wave tetraquark states with positive C -parity, i.e., $J^{PC} = 1^{++}$. Their masses are 3813.1 and 4002.1 MeV. The state with 3813.1 MeV is near the $J/\psi\rho$ and $D\bar{D}^*$ threshold. Thus, it can decay into mesons $\pi^+\pi^-J/\psi$ via the quantum off-shell decay process $\rho \rightarrow \pi^+\pi^-$. The tetraquark states $Qq\bar{Q}\bar{q}$ have no isospin symmetry. However, considering the mixing, different tetraquark states, such as $cu\bar{c}\bar{u}$ and $cu\bar{d}\bar{d}$, can form a state with definite isospin. In particular, the state $|X\rangle = (|cu\bar{c}\bar{u}\rangle - |cu\bar{d}\bar{d}\rangle)/\sqrt{2}$ with $I = 1$ is in good agreement with the experimental results of $X(3872)$ with $I(J^{PC}) = 0(1^{++})$ [3]. However, our predicted mass of 3813.1 MeV is almost 60 MeV lower than 3872 MeV. If this is true, $X(3872)$ is probably a mixed state of excited charmonium ($\chi_{c1}(2P)$) and tetraquark $|X\rangle$ states, which is similar to a mixed molecule-charmonium state [70,71]. Our results are consistent with the conclusions of some previous theoretical studies [72,73]. The 4002.1 MeV is slightly below the $D^*\bar{D}^*$ threshold. It can decay into $D^*\bar{D}^*$ via the off-shell process. Therefore, the possible decay channels are $D^*\bar{D}^*$, $D\bar{D}$, $J/\psi\rho$, and $\eta_c\pi$.

(3) There are two S -wave tetraquark states with

$J^P = 2^+$ ($J^{PC} = 2^{++}$ for charge-neutral states), whose masses are 3852.2 and 4107.5 MeV. The mass of 3852.2 MeV is very close to the $J/\psi\rho$ threshold, and its wave function has a large component of the $J/\psi\rho$ basis ($c_1 = 0.96$). The 4107.5 MeV is above the $D^*\bar{D}^*$ and $J/\psi\rho$ thresholds and may be allowed to decay into $D^*\bar{D}^*$ and $J/\psi\rho$.

2. The $c\bar{s}c\bar{n}$ configuration

The mass spectra of the tetraquark states with the $c\bar{s}c\bar{n}$ configuration are shown in Fig. 1(b). For comparison, we also show the corresponding meson-meson thresholds in this figure. The masses and wave functions amplitudes $\{c_i\}$ are listed in Table 1(b). For the $c\bar{s}c\bar{n}$ state, the C -parity is not a good quantum number. Thus, the quantum numbers of the S -wave tetraquark state $c\bar{s}c\bar{n}$ are $J^P = 0^+, 1^+, \text{ and } 2^+$.

(1) There are four $J^P = 0^+$ states, whose masses are 3455.1, 3857.2, 4078.5, and 4220.8 MeV. The state with the smallest mass, i.e., 3455.1 MeV, is close to the $\eta_c K$ threshold, and its wave function has a large component of the $\eta_c K$ basis ($c_1 = 0.98$). Thus, it can decay into $\eta_c K$ easily. The mass of 3857.2 MeV is above the $\eta_c K$ and $D\bar{D}_s$ thresholds and can naturally decay into mesons $\eta_c K$ and $D\bar{D}_s$. The mass of 4078.5 MeV is below the $D^*\bar{D}_s^*$ threshold but above other possible meson-meson thresholds. The possible decay channels are $\eta_c K$, $D\bar{D}_s$, and $J/\psi K^*$. The state with the largest mass, i.e., 4220.8 MeV, lies above all possible meson-meson thresholds and can decay to $\eta_c K$, $D\bar{D}_s$, $J/\psi K^*$, and $D^*\bar{D}_s^*$.

(2) There are six S -wave tetraquark states with $J^P = 1^+$. Their masses are 3575.6, 3846.6, 3923.8, 4105.5, 4133.2, and 4203.2 MeV. The state with the smallest mass, i.e., 3575.6 MeV, which wave function has a large component of the $J/\psi K$ basis ($c_2 = 0.99$). Because its mass is very close to the $J/\psi K$ threshold, it can

Table 1. Masses (in MeV) and color-spin wave functions (represented by the superposition amplitudes $\{c_i\}$) of the S -wave hidden-charm tetraquark states with quantum numbers $J^{PC} = 0^{+(++)}$, $1^{+(\pm)}$, and $2^{+(++)}$. The labels (a), (b), and (c) correspond to Fig. 1.

System	J^{PC}	Mass	$\{c_i\}$ for $ (Q_1\bar{Q}_3)(q_2\bar{q}_4)\rangle$ basis	$\{c_i\}$ for $ (Q_1\bar{q}_4)(q_2\bar{Q}_3)\rangle$ basis
(a)	$0^{+(++)}$	4146.5	(0.06, -0.16, -0.96, -0.23)	(-0.21, 0.90, 0.25, 0.29)
		3970.9	(0.06, -0.72, -0.05, 0.69)	(-0.37, -0.19, 0.82, 0.39)
		3748.2	(0.11, 0.68, -0.27, 0.67)	(-0.86, -0.24, -0.26, -0.38)
		3109.3	(-0.99, 0.02, -0.09, 0.10)	(-0.30, 0.31, -0.44, 0.79)
	$1^{+(\pm)}$	4125.2	(-0.01, -0.06, 0, -0.45, 0.89, 0)	(0.20, 0.20, -0.88, -0.11, -0.11, 0.35)
		4036.0	(-0.30, -0.08, 0, 0.85, 0.42, 0)	(0.54, 0.54, 0.24, -0.39, -0.39, -0.25)
		3731.7	(-0.95, 0.04, 0, -0.27, -0.13, 0)	(-0.34, -0.34, -0.32, -0.36, -0.36, -0.63)
		3226.8	(-0.02, -0.99, 0, -0.06, -0.09, 0)	(-0.24, -0.24, -0.26, -0.45, -0.45, 0.64)
	$1^{+(++)}$	4002.1	(0, 0, -0.56, 0, 0, 0.83)	(0.42, -0.42, 0, -0.57, 0.57, 0)
		3813.1	(0, 0, -0.83, 0, 0, -0.56)	(-0.57, 0.57, 0, -0.42, 0.42, 0)
	$2^{+(++)}$	4107.5	(-0.28, 0.96)	(-0.81, 0.58)
		3852.2	(-0.96, -0.28)	(-0.58, -0.81)
(b)	0^+	4220.8	(0.08, -0.19, -0.95, -0.24)	(0.19, -0.90, -0.29, 0.29)
		4078.5	(0.08, -0.73, -0.01, 0.68)	(0.33, 0.21, -0.83, -0.39)
		3857.2	(-0.19, -0.65, 0.29, -0.68)	(-0.85, -0.25, -0.20, -0.43)
		3455.1	(-0.98, 0.05, -0.13, 0.17)	(-0.38, 0.30, -0.43, 0.77)
	1^+	4203.2	(-0.03, 0.07, 0.01, 0.56, -0.83, -0.01)	(-0.13, -0.12, 0.90, 0.07, 0.06, -0.39)
		4133.2	(0.32, 0.14, -0.01, -0.78, -0.52, 0.01)	(0.55, 0.53, 0.13, -0.44, -0.43, -0.18)
		4105.5	(-0.001, -0.002, -0.60, 0.02, 0.001, 0.80)	(0.39, -0.40, 0.01, -0.58, 0.59, -0.003)
		3923.8	(0.02, -0.002, 0.80, -0.001, 0.003, 0.60)	(0.59, -0.58, 0.01, 0.40, -0.39, 0.02)
		3846.6	(-0.95, 0.09, 0.01, -0.27, -0.15, 0.01)	(0.33, 0.35, 0.33, 0.33, 0.34, 0.66)
		3575.6	(0.04, 0.99, 0.00, 0.09, 0.14, 0.001)	(-0.28, -0.28, 0.25, -0.45, -0.45, 0.62)
	2^+	4209.2	(-0.29, 0.96)	(-0.80, -0.60)
		3967.2	(-0.96, -0.29)	(0.60, -0.80)
(c)	0^{++}	4302.7	(0.11, -0.24, -0.94, -0.22)	(-0.17, 0.88, 0.34, -0.28)
		4195.1	(0.10, -0.75, 0.05, 0.65)	(0.27, 0.25, -0.84, -0.40)
		3976.5	(-0.35, -0.60, 0.27, -0.67)	(-0.79, -0.29, -0.09, -0.54)
		3739.3	(-0.93, 0.11, -0.21, 0.29)	(-0.53, 0.28, -0.41, 0.69)
	1^{+-}	4289.2	(0.07, -0.08, 0, -0.65, 0.75, 0)	(0.05, 0.05, -0.90, -0.02, -0.02, 0.43)
		4232.3	(-0.34, -0.22, 0, 0.69, 0.60, 0)	(0.51, 0.51, 0.03, -0.48, -0.48, -0.10)
		3975.2	(0.92, -0.25, 0, 0.27, 0.12, 0)	(0.30, 0.30, 0.37, 0.25, 0.25, 0.75)
		3864.9	(-0.16, -0.94, 0, -0.18, -0.24, 0)	(-0.38, -0.38, 0.22, -0.45, -0.45, 0.50)
	1^{++}	4215.2	(0, 0, -0.66, 0, 0, 0.75)	(0.34, -0.34, 0, -0.62, 0.62, 0)
		4039.1	(0, 0, -0.75, 0, 0, -0.66)	(-0.62, 0.62, 0, -0.34, 0.34, 0)
	2^{++}	4309.7	(-0.33, 0.94)	(-0.78, -0.63)
		4092.6	(-0.94, -0.33)	(0.63, -0.78)

decay into $J/\psi K$ with a high probability. Similarly, the mass of 3846.6 MeV can decay into an $\eta_c K$ pair owing to the large fraction $c_1 = 0.95$. The mass of 3923.8 MeV is above the $J/\psi K$ and $\eta_c K^*$ thresholds and close to the $D^* \bar{D}_s$ and $D \bar{D}_s^*$ thresholds. We can see that its wave func-

tion has a large $|\beta_3\rangle$ component ($c_3 = 0.80$), indicating that the meson $\eta_c K^*$ component occupies a large proportion. To study the weights of this state to the $D^* \bar{D}_s$ and $D \bar{D}_s^*$ bases, we convert the tetraquark configuration $|(Q_1\bar{Q}_3)(q_2\bar{q}_4)\rangle$ to $|(Q_1\bar{q}_4)(q_2\bar{Q}_3)\rangle$. As shown in

Table 1, the amplitude of the state (3923.8 MeV) under this set of $|(Q_1\bar{q}_4)(q_2\bar{Q}_3)\rangle$ bases is (0.59, -0.58, 0.01, 0.4, -0.39, 0.02). This suggests that the first two components are approximately the same and relatively large, indicating that the tetraquark state can be allowed to decay into the mesons $D^*\bar{D}_s$ and $D\bar{D}_s^*$. The results nicely explain the nature of the exotic resonant structure $Z_{cs}(3985)^-$ [26]. However, another exotic state $Z_{cs}(4000)^+$, whose mass is very close to $Z_{cs}(3985)^-$ but with a larger decay width, cannot be classified in our calculations. The mass of 4105.5 MeV is only below the $D^*\bar{D}_s^*$ threshold and thus can naturally decay into the mesons $J/\psi K$, $\eta_c K^*$, $J/\psi K^*$, $D^*\bar{D}_s$, and $D\bar{D}_s^*$. The remaining two states 4133.2 and 4203.2 MeV lie above all possible meson-meson thresholds so that all decay modes are possible. In addition, it is worth noting that the mass and decay channel of the tetraquark state 4203.2 MeV with quark content $cu\bar{c}\bar{s}$ is probably the experimentally observed $Z_{cs}(4220)^+$ [27].

(3) For $J^P = 2^+$, masses of two S -wave tetraquark states are 3967.2 and 4209.2 MeV. The lower state lies slightly below the $J/\psi K^*$ threshold, and its wave function has a large component of the $J/\psi K^*$ basis ($c_1 = -0.96$). Thus, it can be searched in the $J/\psi K^*$ channel. The higher state lies above the $J/\psi K^*$ and $D^*\bar{D}_s^*$ thresholds, and its dominant decay modes are mesons $J/\psi K^*$ and $D^*\bar{D}_s^*$.

3. The $cs\bar{c}\bar{s}$ configuration

The tetraquark $cs\bar{c}\bar{s}$ configuration has definite C -parity. The possible quantum numbers are $J^{PC} = 0^{++}$, 1^{+-} , 1^{++} , and 2^{++} . The mass spectra of the tetraquark state with the $cs\bar{c}\bar{s}$ configuration are shown in Fig. 1(c) with corresponding meson-meson thresholds. For the $s\bar{s}$ system, there is no pure spin singlet state, owing to the mixing between $u\bar{u}$ and $d\bar{d}$. For the spin-triplet state, the mixing angle is opportune to form a very nearly pure $s\bar{s}$ state, which is named the ϕ meson. Thus, we only plot the $\eta_c\phi$ and $J/\psi\phi$ thresholds. The superposition amplitudes $\{c_i\}$ of the corresponding tetraquark wave functions are listed in Table 1(c).

(1) There are four S -wave tetraquark states with $J^{PC} = 0^{++}$, whose masses are 3739.3, 3976.5, 4195.1, and 4302.7 MeV. From the wave function of the lowest state, i.e., 3739.3 MeV, we can see that it has a large component based on η_c and the spin singlet state $s\bar{s}$, because $s\bar{s}$ content mixes with $u\bar{u}$ and $d\bar{d}$. Thus, this state may be a superposition of $\eta_c\eta$ and $\eta_c\eta'$. We will not discuss the decay channels of these mixed states in this paper. Considering that its mass is largely below the meson-meson thresholds, it would be a stable tetraquark state. The mass of 3976.5 MeV is close to and above the $D_s\bar{D}_s$ threshold

and thus can naturally decay into mesons $D_s\bar{D}_s$. Now, we convert the $|(Q_1\bar{Q}_3)(q_2\bar{q}_4)\rangle$ configuration into the $|(Q_1\bar{q}_4)(q_2\bar{Q}_3)\rangle$ configuration. Under this set of color-spin bases, the superposition amplitude $\{c_i\}$ of this tetraquark state is (-0.79, -0.29, -0.09, -0.54). It can be found that the amplitude c_1 of the $D_s\bar{D}_s$ component is -0.79. Thus, the main decay channel of this state is mesons $D_s\bar{D}_s$. These analyses indicate that this state probably is the newly observed exotic hadron state $X(3960)$ with $J^{PC} = 0^{++}$. The mass of 4195.1 MeV is above the $D_s\bar{D}_s$ and $J/\psi\phi$ thresholds but below the $D_s^*\bar{D}_s^*$ threshold. Thus, the possible decay channels are $D_s\bar{D}_s$ and $J/\psi\phi$. This state may be the observed $X_0(4140)$ at LHCb [28]. The last state with a mass of 4302.7 MeV is above all possible meson-meson thresholds and can be allowed to decay into $D_s\bar{D}_s$, $D_s^*\bar{D}_s^*$, and $J/\psi\phi$.

(2) There are four S -wave tetraquark states with $J^{PC} = 1^{+-}$, whose masses are 3864.9, 3975.2, 4232.3, and 4289.2 MeV. Without the spin singlet $s\bar{s}$ meson, the lowest state with a mass of 3864.9 MeV is probably a stable tetraquark state. The state of 3975.2 MeV, with a large $\eta_c\phi$ component, can decay into $\eta_c\phi$ via the off-shell process. The two highest states, i.e., 4232.3 and 4289.2 MeV are located above all possible meson-meson thresholds. Considering the conservation of angular momentum and C -parity in the decay process, they can decay into $D_s^*\bar{D}_s^*$ and $D_s\bar{D}_s^*$ via the S wave, because the $D_s\bar{D}_s^*$ pair can form a negative C -parity state via $(D_s\bar{D}_s^* - D_s^*\bar{D}_s)/\sqrt{2}$. Additionally, there are two S -wave tetraquark states with $J^{PC} = 1^{++}$ and masses 4039.1 and 4215.2 MeV, respectively. The state with a mass of 4039.1 MeV has large fractions on both $J/\psi\phi$ and $D_s\bar{D}_s^*$ bases. Satisfying the C -parity conversion, it can decay into $J/\psi\phi$ and a mixed state of $D_s\bar{D}_s^*$ and its antiparticle $(D_s\bar{D}_s^* + D_s^*\bar{D}_s)/\sqrt{2}$. The state of 4215.2 MeV is very close to the $D_s^*\bar{D}_s^*$ threshold. It can decay into $J/\psi\phi$, while the P wave decaying into the final $D_s^*\bar{D}_s^*$ pair is allowed.

(3) For $J^{PC} = 2^{++}$, we find two S -wave tetraquark states with masses of 4092.6 and 4309.7 MeV, respectively. The wave function of 4092.6 MeV has a large $J/\psi\phi$ component, and it can decay into $J/\psi\phi$. The mass of 4309.7 MeV is above all possible meson-meson thresholds and can be allowed to decay into mesons $J/\psi\phi$ and $D_s^*\bar{D}_s^*$.

B. Hidden-bottom tetraquark states with $bn\bar{b}\bar{n}$, $bs\bar{b}\bar{n}$, and $bs\bar{s}\bar{n}$ configurations

The hidden-bottom tetraquark states can be realized by replacing the charm quark in the hidden-charm tetraquark states with the bottom quark. By substituting the corresponding model parameters into Eq. (8), we obtain the mass spectra and wave functions of the S -wave hid-

Table 2. Masses (in MeV) and color-spin wave functions (represented by the superposition amplitudes $\{c_i\}$) of the S -wave hidden-bottom tetraquark states with quantum numbers $J^{PC} = 0^{+(+)}$, $1^{+(\pm)}$, and $2^{+(+)}$. The labels (a), (b), and (c) correspond to Fig. 2.

System	J^{PC}	Mass	$\{c_i\}$ for $ (Q_1\bar{Q}_3)(q_2\bar{q}_4)\rangle$ basis	$\{c_i\}$ for $ (Q_1\bar{q}_4)(q_2\bar{Q}_3)\rangle$ basis
(a)	$0^{+(+)}$	10821.9	(-0.05, 0.01, 0.98, 0.18)	(0.30, -0.88, -0.15, 0.35)
		10688.5	(0.03, -0.17, -0.18, 0.97)	(-0.82, -0.29, 0.47, 0.17)
		10221.4	(0.01, 0.98, -0.04, 0.17)	(-0.44, -0.21, -0.74, -0.46)
		9533.9	(0.99, -0.01, 0.06, -0.02)	(0.21, -0.32, 0.46, -0.80)
	$1^{+(-)}$	10812.2	(0.002, -0.06, 0, -0.20, 0.98, 0)	(0.36, 0.36, -0.77, -0.16, -0.16, 0.32)
		10739.2	(-0.13, -0.02, 0, 0.97, 0.20, 0)	(0.53, 0.53, 0.49, -0.27, -0.27, -0.25)
		10164.9	(0.99, -0.01, 0, 0.12, 0.02, 0)	(0.23, 0.23, 0.30, 0.44, 0.44, 0.64)
		9595.6	(-0.003, -0.998, 0, -0.01, -0.06, 0)	(-0.20, -0.20, 0.27, -0.46, -0.46, 0.65)
	$1^{+(+)}$	10713.7	(0, 0, -0.15, 0, 0, 0.99)	(0.62, -0.62, 0, -0.33, 0.33, 0)
		10224.2	(0, 0, -0.99, 0, 0, -0.15)	(-0.33, 0.33, 0, -0.62, 0.62, 0)
	$2^{+(+)}$	10757.2	(-0.14, 0.99)	(-0.89, -0.45)
		10226.9	(-0.99, -0.14)	(0.45, -0.89)
(b)	0^+	10883.6	(0.07, -0.01, -0.97, -0.23)	(-0.26, 0.88, 0.13, -0.37)
		10776.5	(0.04, -0.19, -0.22, 0.96)	(-0.82, -0.25, 0.49, 0.15)
		10335.7	(0.02, 0.98, -0.05, 0.19)	(-0.46, -0.22, -0.73, -0.46)
		9886.2	(0.99, -0.01, 0.08, -0.03)	(0.23, -0.33, 0.46, -0.79)
	1^+	10874.7	(0.02, -0.07, -0.001, -0.31, 0.95, 0.01)	(-0.30, -0.28, 0.82, 0.13, 0.13, -0.36)
		10827.2	(0.14, 0.04, 0.01, -0.94, -0.31, -0.04)	(0.59, 0.54, 0.40, -0.30, -0.28, -0.21)
		10803.1	(0.01, 0.002, -0.17, -0.03, -0.02, 0.99)	(0.59, -0.64, -0.01, -0.33, 0.36, 0.01)
		10338.9	(0.004, 0, 0.99, 0, -0.001, 0.16)	(0.34, -0.34, 0.001, 0.62, -0.62, 0.003)
		10280.1	(0.99, -0.01, -0.003, 0.13, 0.03, -0.002)	(-0.24, -0.24, -0.31, -0.43, -0.44, -0.64)
		9947.9	(-0.01, -0.99, 0, -0.02, -0.08, 0)	(-0.21, -0.21, 0.28, -0.46, -0.46, 0.65)
	2^+	10847.8	(-0.14, 0.99)	(-0.89, -0.46)
		10342.2	(-0.99, -0.14)	(0.46, -0.89)
(c)	0^{++}	10952.6	(0.09, 0.001, -0.96, -0.27)	(-0.22, 0.89, 0.12, -0.39)
		10864.3	(0.06, -0.22, -0.26, 0.94)	(0.82, 0.21, -0.52, -0.13)
		10460.5	(0.03, 0.98, -0.06, 0.21)	(-0.47, -0.23, -0.71, -0.47)
		10185.2	(0.99, -0.02, 0.10, -0.04)	(-0.25, 0.35, -0.46, 0.78)
	1^{+-}	10945.9	(0.05, -0.09, 0, -0.48, 0.87, 0)	(0.18, 0.18, -0.88, -0.08, -0.08, 0.41)
		10913.0	(-0.15, -0.07, 0, 0.86, 0.48, 0)	(0.60, 0.60, 0.24, -0.33, -0.33, -0.14)
		10406.3	(0.99, -0.03, 0, 0.15, 0.03, 0)	(0.24, 0.24, 0.32, 0.43, 0.43, 0.65)
		10246.7	(-0.02, -0.99, 0, -0.03, -0.11, 0)	(-0.23, -0.23, 0.29, -0.46, -0.46, 0.63)
	1^{++}	10891.9	(0, 0, -0.19, 0, 0, 0.98)	(0.61, -0.61, 0, -0.36, 0.36, 0)
		10464.4	(0, 0, -0.98, 0, 0, -0.19)	(-0.36, 0.36, 0, -0.61, 0.61, 0)
	2^{++}	10937.3	(-0.16, 0.98)	(-0.88, 0.48)
		10468.3	(-0.98, -0.16)	(-0.48, -0.88)

den-bottom tetraquark states. These hidden-bottom tetraquark states can be divided into three configurations: $bn\bar{b}\bar{n}$, $bs\bar{b}\bar{n}$, and $bs\bar{b}\bar{s}$. Their mass spectra and corresponding meson-meson thresholds are presented in Fig. 2. The superposition amplitudes $\{c_i\}$ of the wave functions of

these tetraquark states are listed in Table 2. The analysis method is similar to that for the previous hidden-charm tetraquark states. Thus, we will not discuss them one by one and only focus on two experimental observed states: $Z_b(10610)^+$ and $Z_b(10652)^+$ [25]. They are observed in

the decay channels of $Y(ns)\pi$ and $h_b(mp)\pi$ with $n = 1, 2, 3$ and $m = 1, 2$. Their quantum numbers are probably $J^P = 1^+$ but without the information of the C -parity. In our model, the states with masses of 10713.7 and 10739.2 MeV with $J^P = 1^+$ are probably the observed $Z_b(10610)^+$

and $Z_b(10652)^+$, respectively, as shown in Fig. 2(a). If so, these two states should have different C -parities. Their wave function has a very large fraction on the β_4 and β_6 bases, which indicates these two states may be the diquark-antiquark bound states.

Table 3. Masses (in MeV) and color-spin wave functions (represented by the superposition amplitudes $\{c_i\}$) of the S -wave mixed-charm-bottom tetraquark states with quantum numbers $J^P = 0^+$, 1^+ , and 2^+ . The labels (a), (b), and (c) correspond to Fig. 3.

System	J^P	Mass	$\{c_i\}$ for $ (Q_1\bar{Q}_3)(q_2\bar{q}_4)\rangle$ basis	$\{c_i\}$ for $ (Q_1\bar{q}_4)(q_2\bar{Q}_3)\rangle$ basis
(a)	0^+	7471.9	(-0.06, 0.07, 0.97, 0.23)	(0.24, -0.90, -0.18, 0.33)
		7303.8	(0.06, -0.46, -0.17, 0.87)	(-0.65, -0.21, 0.68, 0.26)
		7069.5	(0.05, 0.89, -0.16, 0.43)	(-0.68, -0.23, -0.55, -0.43)
		6406.2	(0.99, -0.02, 0.08, -0.06)	(0.25, -0.32, 0.45, -0.80)
	1^+	7461.8	(-0.01, -0.06, 0.02, -0.27, 0.95, 0.14)	(0.41, 0.21, -0.80, -0.17, -0.13, 0.32)
		7401.3	(-0.18, -0.03, -0.12, 0.83, 0.16, 0.49)	(0.73, 0.13, 0.41, -0.46, -0.07, -0.26)
		7322.6	(0.15, 0.05, -0.35, -0.43, -0.23, 0.79)	(0.17, -0.72, -0.11, -0.21, 0.62, 0.12)
		7088.7	(0.14, 0.02, 0.93, -0.03, -0.07, 0.34)	(0.43, -0.47, 0.06, 0.63, -0.44, 0.07)
		7030.0	(0.96, -0.03, -0.10, 0.23, 0.09, -0.08)	(0.23, 0.38, 0.33, 0.34, 0.44, 0.63)
		6477.1	(0.01, 0.99, -0.01, 0.04, 0.08, -0.03)	(0.20, 0.24, -0.26, 0.46, 0.45, -0.65)
	2^+	7424.9	(-0.22, 0.98)	(-0.85, -0.53)
		7105.1	(-0.98, -0.22)	(0.53, -0.85)
(b)	0^+	7544.2	(-0.08, 0.07, 0.96, 0.26)	(0.21, -0.90, -0.18, 0.35)
		7404.5	(0.08, -0.49, -0.19, 0.85)	(-0.63, -0.19, 0.72, 0.25)
		7182.0	(0.09, 0.87, -0.18, 0.45)	(-0.69, -0.23, -0.51, -0.46)
		6756.7	(0.99, -0.03, 0.10, -0.09)	(0.29, -0.32, 0.45, -0.78)
	1^+	7535.8	(-0.01, 0.08, -0.02, 0.38, -0.91, -0.13)	(-0.33, -0.15, 0.84, 0.14, 0.10, -0.36)
		7499.5	(-0.19, -0.05, -0.12, 0.79, 0.25, 0.52)	(0.77, 0.14, 0.32, -0.49, -0.08, -0.22)
		7421.1	(0.17, 0.08, -0.37, -0.42, -0.27, 0.76)	(0.13, -0.71, -0.08, -0.19, 0.66, 0.09)
		7203.3	(0.16, 0.04, 0.91, -0.03, -0.08, 0.36)	(0.44, -0.47, 0.07, 0.64, -0.41, 0.07)
		7145.4	(0.96, -0.05, -0.12, 0.23, 0.10, -0.09)	(0.22, 0.40, 0.33, 0.32, 0.43, 0.64)
		6827.9	(0.02, 0.99, -0.02, 0.05, 0.11, -0.05)	(0.21, 0.28, -0.27, 0.45, 0.45, -0.63)
	2^+	7524.4	(-0.23, 0.97)	(-0.84, -0.54)
		7221.2	(-0.97, -0.23)	(0.54, -0.84)
(c)	0^+	7615.1	(-0.11, 0.08, 0.95, 0.27)	(0.19, -0.89, -0.20, 0.37)
		7507.2	(0.12, -0.56, -0.17, 0.80)	(-0.55, -0.18, 0.77, 0.26)
		7297.1	(0.17, 0.82, -0.20, 0.51)	(-0.72, -0.27, -0.41, -0.50)
		7049.8	(0.97, -0.07, 0.16, -0.16)	(0.39, -0.33, 0.44, -0.74)
	1^+	7609.7	(-0.07, 0.10, -0.05, 0.56, -0.82, -0.03)	(-0.15, -0.08, 0.88, 0.04, 0.08, -0.44)
		7588.7	(-0.21, -0.09, -0.15, 0.66, 0.44, 0.54)	(0.80, 0.15, 0.12, -0.55, -0.10, -0.13)
		7519.9	(0.19, 0.12, -0.43, -0.41, -0.29, 0.72)	(0.10, -0.65, -0.07, -0.19, 0.72, 0.07)
		7322.4	(0.19, 0.08, 0.88, -0.02, -0.08, 0.42)	(0.49, -0.49, 0.07, 0.63, -0.34, 0.06)
		7269.2	(0.94, -0.13, -0.13, 0.26, 0.10, -0.11)	(0.20, 0.41, 0.36, 0.26, 0.38, 0.67)
		7121.2	(0.07, 0.97, -0.05, 0.10, 0.18, -0.09)	(0.24, 0.38, -0.27, 0.44, 0.46, -0.58)
	2^+	7617.1	(-0.27, 0.96)	(-0.82, -0.57)
		7344.9	(-0.96, -0.27)	(0.57, -0.82)

C. Tetraquark states with $bn\bar{c}\bar{n}$, $bs\bar{c}\bar{n}$, and $bs\bar{c}\bar{s}$ configurations

The mixed charm-bottom tetraquark state can be obtained by substituting a charm quark in the hidden-charm tetraquark state with a bottom quark or by substituting a bottom quark in the hidden-bottom tetraquark state with a charm quark. The difference, however, is that these configurations break the charge conjugation symmetry. Hence, the quantum numbers for the charm-bottom tetraquark systems, i.e., $bn\bar{c}\bar{n}$, $bs\bar{c}\bar{n}$, and $bs\bar{c}\bar{s}$, are $J^P = 0^+$, 1^+ , and 2^+ . Similarly, we can obtain their masses and wave functions by using the ICMI model. Our theoretical results are shown in Fig. 3 and Table 3. The analysis method is similar to that for the previous hidden-charm tetraquark states.

IV. SUMMARY

In this work, we complete a systematic study of the S -wave tetraquark states $Qq\bar{Q}\bar{q}$ ($Q = c, b$ and $q = u, d, s$) via the ICMI model, which includes both the chromomagnetic and chromoelectric interactions. The parameters in the ICMI model are obtained by fitting the known hadron spectra, and they are taken directly from the previous work [60]. The mass spectra, possible decay channels, and inner structures of the S -wave tetraquark $Qq\bar{Q}\bar{q}$ with quantum numbers $J^{PC} = 0^{+(+)}$, $1^{+(\pm)}$, and $2^{+(+)}$ are presented and analyzed. For the charge-neutral tetraquark state, the charge conjugation is also considered when analyzing the possible decay channels.

The recently observed hidden-charm tetraquark states, such as $Z_{cs}(3985)^-$, $X(3960)$, and $Z_{cs}(4220)^+$, can be well explained in our model. The tetraquark state $cs\bar{c}\bar{u}$ with mass 3923.8 MeV and the quantum number $J^P = 1^+$ can be considered as a good candidate for $Z_{cs}(3985)^-$. For the $cs\bar{c}\bar{s}$ configuration, we find a tetraquark state with a mass of 3976.5 MeV and a quantum number of $J^{PC} = 0^{++}$. The properties of this state are in good agreement with $X(3960)$. Meanwhile, according to the wave functions of each S -wave tetraquark $Qq\bar{Q}\bar{q}$, we find that the low-lying states in each configuration have a significant component of the $|(Q_1\bar{Q}_3)^1(q_2\bar{q}_4)^1\rangle$ basis (the probability $|c_i|^2 > 90\%$), as shown in Table 4. This indicates they have a large probability to decay into $Q\bar{Q}$ and $q\bar{q}$ mesons instead of $Q\bar{q}$ and $q\bar{Q}$ mesons. In some sense, these states are probably the molecule states of $Q\bar{Q}$ and $q\bar{q}$. Of course, other evidence, such as the mean radius and hadron level inter-

Table 4. Tetraquark states, which have a large overlap ($|c_i|^2 > 90\%$) to the $Q\bar{Q}$ and $q\bar{q}$ mesons. Their masses (in MeV), quantum numbers, and meson-meson contents are listed. B_c^* with $J^P = 1^-$ has not been found in experiments.

System	J^P	Mass	Meson-Meson
$cn\bar{c}\bar{n}$	0^+	3109.3	$\eta_c\pi$
$cn\bar{c}\bar{n}$	1^+	3226.8	$J/\psi\pi$
$cn\bar{c}\bar{n}$	1^+	3731.7	$\eta_c\rho$
$cn\bar{c}\bar{n}$	2^+	3852.2	$J/\psi\rho$
$cs\bar{c}\bar{n}$	0^+	3455.1	$\eta_c K$
$cs\bar{c}\bar{n}$	1^+	3575.6	$J/\psi K$
$cs\bar{c}\bar{n}$	1^+	3846.6	$\eta_c K^*$
$cs\bar{c}\bar{n}$	2^+	3967.2	$J/\psi K^*$
$bn\bar{b}\bar{n}$	0^+	9533.9	$\eta_b\pi$
$bn\bar{b}\bar{n}$	1^+	9595.6	$\Upsilon\pi$
$bn\bar{b}\bar{n}$	1^+	10164.9	$\eta_b\rho$
$bn\bar{b}\bar{n}$	1^+	10224.2	$\Upsilon\rho$
$bn\bar{b}\bar{n}$	2^+	10226.9	$\Upsilon\rho$
$bs\bar{b}\bar{n}$	0^+	9886.2	$\eta_b K$
$bs\bar{b}\bar{n}$	1^+	9947.9	ΥK
$bs\bar{b}\bar{n}$	1^+	10280.1	$\eta_b K^*$
$bs\bar{b}\bar{n}$	1^+	10338.9	ΥK^*
$bs\bar{b}\bar{n}$	2^+	10342.2	ΥK^*
$bs\bar{b}\bar{s}$	1^+	10406.3	$\eta_b\phi$
$bs\bar{b}\bar{s}$	1^+	10464.4	$\Upsilon\phi$
$bs\bar{b}\bar{s}$	2^+	10468.3	$\Upsilon\phi$
$bn\bar{c}\bar{n}$	0^+	6406.2	$B_c\pi$
$bn\bar{c}\bar{n}$	1^+	6477.1	$B_c^*\pi$
$bn\bar{c}\bar{n}$	1^+	7030.0	$B_c\rho$
$bn\bar{c}\bar{n}$	2^+	7105.1	$B_c^*\rho$
$bs\bar{c}\bar{n}$	0^+	6756.7	$B_c K$
$bs\bar{c}\bar{n}$	1^+	6827.9	$B_c^* K$
$bs\bar{c}\bar{n}$	1^+	7145.4	$B_c K^*$
$bs\bar{c}\bar{n}$	2^+	7221.2	$B_c^* K^*$
$bs\bar{c}\bar{s}$	2^+	7344.9	$B_c^*\phi$

actions, is needed to determine whether they are molecular states [74–78]. Our predictions regarding these exotic tetraquark states $Qq\bar{Q}\bar{q}$ can be examined in future experiments.

References

- [1] R. Aaij *et al.* (LHCb), *Phys. Rev. Lett.* **125**, 242001 (2020), arXiv:2009.00025[hep-ex]
- [2] R. Aaij *et al.* (LHCb), *Nature Phys.* **18**, 751 (2022), arXiv:2109.01038[hep-ex]
- [3] S. K. Choi *et al.* (Belle), *Phys. Rev. Lett.* **91**, 262001 (2003), arXiv:hep-ex/0309032
- [4] H.-X. Chen, W. Chen, X. Liu *et al.*, *Phys. Rept.* **639**, 1 (2016), arXiv:1601.02092[hep-ph]
- [5] A. Esposito, A. Pilloni, and A. D. Polosa, *Phys. Rept.* **668**, 1 (2017), arXiv:1611.07920[hep-ph]

- [6] M. Karliner, J. L. Rosner, and T. Skwarnicki, *Ann. Rev. Nucl. Part. Sci.* **68**, 17 (2018), arXiv:1711.10626[hep-ph]
- [7] F.-K. Guo, C. Hanhart, U.-G. Meißner *et al.*, *Rev. Mod. Phys.* **90**, 015004 (2018), arXiv:1705.00141[hepph]
- [8] N. Brambilla, S. Eidelman, C. Hanhart *et al.*, *Phys. Rept.* **873**, 1 (2020), arXiv:1907.07583[hep-ex]
- [9] Q. Wang, C. Hanhart, and Q. Zhao, *Phys. Rev. Lett.* **111**, 132003 (2013), arXiv:1303.6355[hep-ph]
- [10] F. E. Close and P. R. Page, *Nucl. Phys. B* **443**, 233 (1995), arXiv:hep-ph/9411301
- [11] R. Onocala and J. Soto, *Phys. Rev. D* **96**, 014004 (2017), arXiv:1702.03900[hep-ph]
- [12] T. F. Carames, A. Valcarce, and J. Vijande, *Phys. Lett. B* **709**, 358 (2012), arXiv:1203.1123[hep-ph]
- [13] D.-Y. Chen, X. Liu, and T. Matsuki, *Phys. Rev. Lett.* **110**, 232001 (2013), arXiv:1303.6842[hep-ph]
- [14] E. S. Swanson, *Phys. Rev. D* **91**, 034009 (2015), arXiv:1409.3291[hep-ph]
- [15] S. X. Nakamura, *Phys. Rev. D* **102**, 074004 (2020), arXiv:1912.11830[hep-ph]
- [16] F.-K. Guo, X.-H. Liu, and S. Sakai, *Prog. Part. Nucl. Phys.* **112**, 103757 (2020), arXiv:1912.07030[hep-ph]
- [17] E. Braaten, L.-P. He, and K. Ingle, *Phys. Rev. D* **100**, 031501 (2019), arXiv:1904.12915[hep-ph]
- [18] T.-W. Chiu and T.-H. Hsieh (TWQCD), *Phys. Rev. D* **73**, 111503 (2006) [Erratum: *Phys. Rev. D* **75**, 019902 (2007)] arXiv: hep-lat/0604008
- [19] M. Ablikim *et al.* (BESIII), *Phys. Rev. Lett.* **110**, 252001 (2013), arXiv:1303.5949[hep-ex]
- [20] Z. Q. Liu *et al.* (Belle), *Phys. Rev. Lett.* **110**, 252002 (2013), arXiv:1304.0121[hep-ex]
- [21] M. Ablikim *et al.* (BESIII), *Phys. Rev. Lett.* **112**, 132001 (2014), arXiv:1308.2760[hep-ex]
- [22] R. Aaij *et al.* (LHCb), *Eur. Phys. J. C* **78**, 1019 (2018), arXiv:1809.07416[hep-ex]
- [23] S. K. Choi *et al.* (Belle), *Phys. Rev. Lett.* **100**, 142001 (2008), arXiv:0708.1790[hep-ex]
- [24] R. Aaij *et al.* (LHCb), *Phys. Rev. Lett.* **112**, 222002 (2014), arXiv:1404.1903[hep-ex]
- [25] A. Bondar *et al.* (Belle), *Phys. Rev. Lett.* **108**, 122001 (2012), arXiv:1110.2251[hep-ex]
- [26] M. Ablikim *et al.* (BESIII), *Phys. Rev. Lett.* **126**, 102001 (2021), arXiv:2011.07855[hep-ex]
- [27] R. Aaij *et al.* (LHCb), *Phys. Rev. Lett.* **127**, 082001 (2021), arXiv:2103.01803[hep-ex]
- [28] R. Aaij *et al.* (LHCb), (2022), arXiv: 2210.15153[hep-ex]
- [29] E. Braaten, C. Langmack, and D. H. Smith, *Phys. Rev. D* **90**, 014044 (2014), arXiv:1402.0438[hep-ph]
- [30] J. Vijande, E. Weissman, N. Barnea *et al.*, *Phys. Rev. D* **76**, 094022 (2007), arXiv:0708.3285[hep-ph]
- [31] J. Vijande, E. Weissman, A. Valcarce *et al.*, *Phys. Rev. D* **76**, 094027 (2007), arXiv:0710.2516[hep-ph]
- [32] T. Fernandez-Carames, A. Valcarce, and J. Vijande, *Phys. Rev. Lett.* **103**, 222001 (2009), arXiv:1001.4506[hep-ph]
- [33] G. Yang, J. Ping, and J. Segovia, *Phys. Rev. D* **104**, 094035 (2021), arXiv:2109.04311[hep-ph]
- [34] R. Tiwari and A. K. Rai, (2022), arXiv: 2206.04478[hep-ph]
- [35] W. Chen, H.-X. Chen, X. Liu *et al.*, *Phys. Rev. D* **96**, 114017 (2017), arXiv:1706.09731[hep-ph]
- [36] Q. Xin, Z.-G. Wang, and X.-S. Yang, (2022), arXiv: 2207.09910[hep-ph]
- [37] G. S. Bali, S. Collins, and C. Ehm, *Phys. Rev. D* **84**, 094506 (2011), arXiv:1110.2381[hep-lat]
- [38] S. Prelovsek and L. Leskovec, *Phys. Rev. Lett.* **111**, 192001 (2013), arXiv:1307.5172[hep-lat]
- [39] M. Sadl and S. Prelovsek, *Phys. Rev. D* **104**, 114503 (2021), arXiv:2109.08560[hep-lat]
- [40] C. Hidalgo-Duque, J. Nieves, and M. P. Valderrama, *Phys. Rev. D* **87**, 076006 (2013), arXiv:1210.5431[hep-ph]
- [41] H.-W. Ke, Z.-T. Wei, and X.-Q. Li, *Eur. Phys. J. C* **73**, 2561 (2013), arXiv:1307.2414[hep-ph]
- [42] M. Cleven, Q. Wang, F.-K. Guo *et al.*, *Phys. Rev. D* **87**, 074006 (2013), arXiv:1301.6461[hep-ph]
- [43] X.-K. Dong, F.-K. Guo, and B.-S. Zou, *Progr. Phys.* **41**, 65 (2021), arXiv:2101.01021[hep-ph]
- [44] Y.-H. Ge, X.-H. Liu, and H.-W. Ke, *Eur. Phys. J. C* **81**, 854 (2021), arXiv:2103.05282[hep-ph]
- [45] R. Chen and Q. Huang, (2022), arXiv: 2209.05180[hep-ph]
- [46] J. Wu, X. Liu, Y.-R. Liu *et al.*, *Phys. Rev. D* **99**, 014037 (2019), arXiv:1810.06886[hep-ph]
- [47] B. Silvestre-Brac, *Phys. Rev. D* **46**, 2179 (1992)
- [48] F. Buccella, H. Høgaasen, J.-M. Richard *et al.*, *Eur. Phys. J. C* **49**, 743 (2007), arXiv:hep-ph/0608001
- [49] H. Høgaasen and P. Sorba, *Mod. Phys. Lett. A* **19**, 2403 (2004), arXiv:hep-ph/0406078
- [50] Y. Cui, X.-L. Chen, W.-Z. Deng *et al.*, *Phys. Rev. D* **73**, 014018 (2006), arXiv:hep-ph/0511150
- [51] L. Maiani, F. Piccinini, A. D. Polosa *et al.*, *Phys. Rev. Lett.* **93**, 212002 (2004), arXiv:hep-ph/0407017
- [52] F. Stancu, *J. Phys. G* **37**, 075017 (2010) [Erratum: *J. Phys. G* **46**, 019501 (2019)], arXiv: 0906.2485[hep-ph]
- [53] T. Guo, L. Cao, M.-Z. Zhou *et al.*, (2011), arXiv: 1106.2284[hep-ph]
- [54] S.-Q. Luo, K. Chen, X. Liu *et al.*, *Eur. Phys. J. C* **77**, 709 (2017), arXiv:1707.01180[hep-ph]
- [55] J. Wu, Y.-R. Liu, K. Chen *et al.*, *Phys. Rev. D* **95**, 034002 (2017), arXiv:1701.03873[hep-ph]
- [56] J.-B. Cheng, S.-Y. Li, Y.-R. Liu *et al.*, *Phys. Rev. D* **101**, 114017 (2020), arXiv:2001.05287[hep-ph]
- [57] H. Høgaasen, E. Kou, J.-M. Richard *et al.*, *Phys. Lett. B* **732**, 97 (2014), arXiv:1309.2049[hep-ph]
- [58] X.-Z. Weng, X.-L. Chen, and W.-Z. Deng, *Phys. Rev. D* **97**, 054008 (2018), arXiv:1801.08644[hep-ph]
- [59] H.-T. An, K. Chen, Z.-W. Liu *et al.*, *Phys. Rev. D* **103**, 114027 (2021), arXiv:2106.02837[hep-ph]
- [60] T. Guo, J. Li, J. Zhao, and L. He, *Phys. Rev. D* **105**, 054018 (2022), arXiv:2108.06222[hep-ph]
- [61] T. Guo, J. Li, J. Zhao, and L. He, *Phys. Rev. D* **105**, 014021 (2022), arXiv:2108.10462[hep-ph]
- [62] X.-Z. Weng, W.-Z. Deng, and S.-L. Zhu, *Chin. Phys. C* **46**, 013102 (2022), arXiv:2108.07242[hep-ph]
- [63] X.-Z. Weng, X.-L. Chen, W.-Z. Deng *et al.*, *Phys. Rev. D* **100**, 016014 (2019), arXiv:1904.09891[hep-ph]
- [64] X.-Z. Weng, X.-L. Chen, W.-Z. Deng *et al.*, *Phys. Rev. D* **103**, 034001 (2021), arXiv:2010.05163[hep-ph]
- [65] H.-T. An, Z.-W. Liu, F.-S. Yu *et al.*, (2022), arXiv: 2207.02813[hep-ph]
- [66] X.-Z. Weng and S.-L. Zhu, (2022), arXiv: 2207.05505[hep-ph]
- [67] Z. Liu, H.-T. An, Z.-W. Liu *et al.*, (2022), arXiv: 2209.10440[hep-ph]
- [68] A. De Rujula, H. Georgi, and S. L. Glashow, *Phys. Rev. D* **12**, 147 (1975)
- [69] M. Oka and S. Takeuchi, *Phys. Rev. Lett.* **63**, 1780 (1989)
- [70] A. M. Badalian, V. D. Orlovsky, Y. A. Simonov *et al.*,

- [71] [Phys. Rev. D **85**, 114002 \(2012\)](#), arXiv:1202.4882[hep-ph]
R. D. Matheus, F. S. Navarra, M. Nielsen *et al.*, [Phys. Rev. D **80**, 056002 \(2009\)](#), arXiv:0907.2683[hep-ph]
- [72] L. Maiani, F. Piccinini, A. D. Polosa *et al.*, [Phys. Rev. D **71**, 014028 \(2005\)](#), arXiv:hep-ph/0412098
- [73] H. Hogaasen, J. M. Richard, and P. Sorba, [Phys. Rev. D **73**, 054013 \(2006\)](#), arXiv:hep-ph/0511039
- [74] M. B. Voloshin, (2006), arXiv: [hep-ph/0602233](#)
- [75] Y.-J. Zhang, H.-C. Chiang, P.-N. Shen *et al.*, [Phys. Rev. D **74**, 014013 \(2006\)](#), arXiv:hep-ph/0604271
- [76] X. Liu, Z.-G. Luo, Y.-R. Liu *et al.*, [Eur. Phys. J. C **61**, 411 \(2009\)](#), arXiv:0808.0073[hep-ph]
- [77] X.-K. Dong, V. Baru, F.-K. Guo *et al.*, [Sci. Bull. **66**, 2462 \(2021\)](#), arXiv:2107.03946[hepph]
- [78] K. Chen, R. Chen, L. Meng *et al.*, [Eur. Phys. J. C **82**, 581 \(2022\)](#), arXiv:2109.13057[hep-ph]